Biochemical and Biophysical Research Communications 394 (2010) 130–135

Contents lists available at ScienceDirect

Biochemical and Biophysical Research Communications

journal homepage: www.elsevier.com/locate/ybbrc

Exchange of rotor components in functioning bacterial flagellar motor

Hajime Fukuoka [a,b], Yuichi Inoue [a,b], Shun Terasawa [b], Hiroto Takahashi [a], Akihiko Ishijima [a,b,*]

[a] Institute of Multidisciplinary Research for Advanced Materials, Tohoku University, Aoba-ku, Sendai 980-8577, Japan
[b] Graduate School of Life Sciences, Tohoku University, Aoba-ku, Sendai 980-8577, Japan

ARTICLE INFO

Article history:
Received 18 February 2010
Available online 23 February 2010

Keywords:
Molecular motor
Bacterial flagella
TIRF
FRAP
GFP
E. coli

ABSTRACT

The bacterial flagellar motor is a rotary motor driven by the electrochemical potential of a coupling ion. The interaction between a rotor and stator units is thought to generate torque. The overall structure of flagellar motor has been thought to be static, however, it was recently proved that stators are exchanged in a rotating motor. Understanding the dynamics of rotor components in functioning motor is important for the clarifying of working mechanism of bacterial flagellar motor. In this study, we focused on the dynamics and the turnover of rotor components in a functioning flagellar motor. Expression systems for GFP-FliN, FliM-GFP, and GFP-FliG were constructed, and each GFP-fusion was functionally incorporated into the flagellar motor. To investigate whether the rotor components are exchanged in a rotating motor, we performed fluorescence recovery after photobleaching experiments using total internal reflection fluorescence microscopy. After photobleaching, in a tethered cell producing GFP-FliN or FliM-GFP, the recovery of fluorescence at the rotational center was observed. However, in a cell producing GFP-FliG, no recovery of fluorescence was observed. The transition phase of fluorescence intensity after full or partially photobleaching allowed the turnover of FliN subunits to be calculated as 0.0007 s^{-1}, meaning that FliN would be exchanged in tens of minutes. These novel findings indicate that a bacterial flagellar motor is not a static structure even in functioning state. This is the first report for the exchange of rotor components in a functioning bacterial flagellar motor.

1. Introduction

The bacterial flagellum is a supramolecular complex and functions as rotary motor driven by the flux of H^+ or Na^+ [1–5]. A feature of the torque-speed relationships is common between H^+- and Na^+-driven motors [6–8]. Flagellum consists of a basal body (rotary motor), a helical filament (propeller) and a hook connecting them. The motor consists of a rotor and some stator units; a stator unit is thought to be a torque generator that converts the energy of ion flux into mechanical power.

The stator part consists of several units, at least 11 in *Escherichia coli* [9]. Stator unit is thought to consist of 4 molecules of A-subunits and 2 molecules of B-subunits [10]. The B subunit contains a large periplasmic domain that has a putative peptidoglycan-binding domain, and the assembly of stator units to the motor requires this domain [11]. In *Salmonella*, a crystal structure of this domain has been solved and a model for stator assembly was proposed [12]. The basal body of Gram-negative bacteria consists of a rod and several rings, termed the L-, P-, MS-, and C-ring (Fig. 1A) [2]. During flagellar assembly, 26 copies of FliF multimerizes to form the MS-ring and 26 copies of FliG are thought to attach to the MS-ring. 34 copies of FliM and more than 100 copies of FliN assemble to form the main structure of the C-ring. FliG is thought to interact with charged residues in the cytoplasmic domain of the stator protein MotA to generate torque [13]. FliM has a sequence for binding the chemotaxis signaling molecule, phosphorylated CheY, in its N-terminal domain [14]. By binding of phosphorylated CheY, rotational direction of motor is changed from counter-clockwise (CCW) to clockwise (CW). FliN interacts with the C-terminal domain of FliM, which shows sequence homology to FliN [15]. FliG, FliM and FliN are involved in the formation of flagellar structure, the rotation of motor, and the switching of rotational direction [2].

The overall structure of flagellar motor has been investigated well. The flagellar structure has been thought to be static after its assembly is completed. However, it was recently proved that stator of flagellar motor is dynamic [5,16,17]. Understanding the dynamics of components in functioning state is important for the clarifying of working mechanism of supramolecular machines. Therefore, we have focused on the dynamics and turnover of rotor subunits, and demonstrated that the rotor components, FliN and FliM, are exchanged in a functioning motor. This is the first evidence for the exchange of rotor components in a functioning bacterial flagellar motor.

* Corresponding author. Address: Institute of Multidisciplinary Research for Advanced Materials, Tohoku University, Aoba-ku, Sendai 980-8577, Japan. Fax: +81 22 217 5802.
E-mail address: ishijima@tagen.tohoku.ac.jp (A. Ishijima).

0006-291X/$ - see front matter © 2010 Elsevier Inc. All rights reserved.
doi:10.1016/j.bbrc.2010.02.129

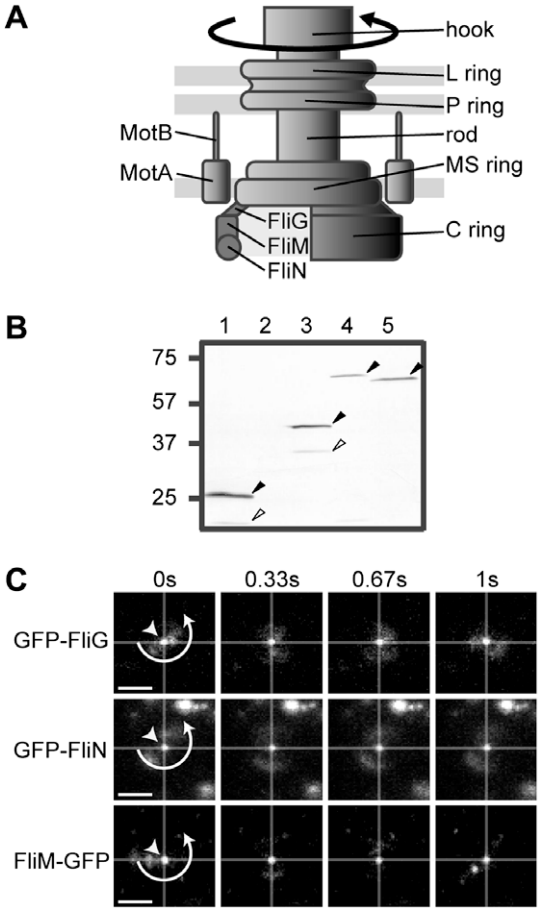

Fig. 1. (A) Diagram of *E. coli* flagellar motor. (B) Immunoblots for GFP-fusions from whole-cell extracts. Molecular mass values (kD) were shown on the left side of the panel. Black arrowheads correspond to mature GFP or GFP-fusions. White arrowheads indicate the bands smaller than the expected mature size. Lane 1–3 indicate the bands from EFS021 producing GFP, wild-type FliN and GFP-FliN, respectively. Lane 4 indicates the band from EFS011 cells producing FliM-GFP. Lane 5 indicates the band from DFB225 cells producing GFP-FliG. (C) Sequential images of tethered cells producing GFP-fusions. Fluorescent images were shown every 1/3 s. Top, DFB225 cell producing GFP-FliG; middle, EFS021 cell producing GFP-FliN; bottom, EFS011 cell producing FliM-GFP. White arrowheads and circular arrows indicate fluorescent spots localizing at the rotational center and the rotational direction of tethered cell, respectively. Scale bar, 1.6 μm.

2. Materials and methods

2.1. Bacterial strains and plasmids

Bacterial strains and plasmids were shown in Supplementary materials. LB broth (1% bactotryptone, 0.5% yeast extract, 0.5% NaCl) was used for culture growth, transformations, and plasmid isolation. T broth (1% bactotryptone, 0.5% NaCl) was used for cell growth in motility assay and in the observation by fluorescence microscopy. Arabinose was added to T broth to be 0.002%, 0.005%, and 0.0005% to produce GFP-FliN, FliM-GFP, and GFP-FliG, respectively.

2.2. Cell preparation for the observation by fluorescence microscopy

Overnight cultures were inoculated into T broth (1/100 volume) containing appropriate concentration of arabinose and cells were grown for 4.5–5 h at 30 °C. For the observation of GFP-FliN, EFS021 strain (Δ*fliN*) harboring pFSGN3 (*gfp-fliN*) and pYS11 (*fliC-sticky*), and EFS022 (Δ*fliN fliC-sticky*) strain harboring pFSGN3 were used. For the observation of FliM-GFP, EFS011 (Δ*fli*M) strain harboring pFS6003m (*fliM-gfp*) and pFSST1 (*fliC-sticky*), and EFS012 (Δ*fli*M *fliC-sticky*) strain harboring pFS6003m were used. For the observation of GFP-FliG, DFB225 strain (Δ*fliG*) harboring pTH2100 (*gfp-fliG*) and pYS11 was used.

To shorten flagellar filaments, cells were passed through a narrow polystyrene tube connected between two syringes more than 40 times. Cells were harvested by centrifugation and resuspended in 85NaMB (10 mM potassium phosphate (pH 7.0), 85 mM NaCl, 0.1 mM EDTA). The cell suspension was incubated for 10 min at room temperature. The cell suspension was loaded into the space between a coverslip and a microscope slide with a spacer to stuck the cells on a coverslip spontaneously. Additional 85NaMB was loaded to remove the unattached cells, and the sample was incubated for 10 min at room temperature. Cells were observed under the Olympus IX71 based Total Internal Reflection Fluorescence (TIRF) microscopy [18] and images were recorded at 30.25 frames/s using EMCCD camera (DU860-BV, Andor Technology, UK).

2.3. FRAP experiment by TIRF microscopy

Fluorescence Recovery After Photobleaching (FRAP) experiment were performed using TIRF microscopy. By removing ND filter (13%) from the optical axis, tethered cells were irradiated with high intensity evanescent light and the fluorescent spot at the rotational center, which locates near glass surface (∼50 nm), was completely or partially photobleached.

2.4. Measurement of fluorescence intensity

To estimate the fluorescence intensity of a fluorescent spot, two-dimensional Gaussian function was applied to the images of single fluorescent spot using self-made program constructed by Labview ver. 8.6 (National Instruments, USA). We defined the peak value from Gaussian fit as fluorescence intensity of each spot.

2.5. Swimming speed of the cell producing GFP-fusion

Cell cultures were diluted with 85NaMB containing 20 mM serine, to suppress the change of rotational direction of motor. Swimming behavior of cells was recorded on videotape and the swimming speed was calculated on the monitor.

2.6. Measurement of rotational speed and CCW bias of motor

Cell suspension was loaded into the space between coverslips with a spacer, and was incubated for 10 min. Additional 85NaMB was loaded to remove the unattached cells on the coverslip. The suspension of polystyrene beads (φ = 0.5 μm) was loaded and sample slide was incubated for 10 min to attach bead to flagellar filament. Additional 85NaMB was loaded to remove the unattached beads. The phase contrast image of bead on flagella filament was recorded by high speed CCD camera (IPX-VGA210LMCN, IMPERX, USA) at 1250 frames/s. Image of bead was fitted by two-dimensional Gaussian function to estimate the position of bead. The angular velocity and CCW bias were calculated using self-made programs constructed by Labview ver. 8.6.

2.7. Immunoblotting for the GFP-fusions

The cells were harvested by centrifugation and condensed by sterilized water (optical density at 660 nm, 20). Cell suspensions were diluted by the same volume of 5× SDS loading buffer containing β-mercaptoethanol and were boiled at 100 °C for 5 min. The proteins were separated by SDS–PAGE and immunoblotting was performed using anti-GFP antibody (Clontech, USA). Bands were

Table 1
Cell motility and function of motor.

Rotor subunit	Swimming speed (μm/s)[a]	Rotational speed (Hz)[b]	CCW bias[c]	Fluorescence intensity[d]
GFP-FliN	27.6 ± 2.5 (n = 20)	83.2 ± 11.4 (n = 13)	0.67 ± 0.09 (n = 13)	7823 ± 1183 (n = 40)
Wild-type FliN	29.8 ± 1.6 (n = 20)	84.0 ± 12.2 (n = 14)	0.61 ± 0.16 (n = 14)	–
FliM-GFP	25.9 ± 2.0 (n = 20)	75.7 ± 28.6 (n = 26)	0.58 ± 0.14 (n = 26)	2194 ± 350 (n = 40)
Wild-type FliM	30.9 ± 3.1 (n = 20)	82.8 ± 6.8 (n = 11)	0.72 ± 0.06 (n = 11)	–

n is the total number of cells that were analyzed. Values were shown as mean ± SD.
[a] To measure swimming speeds, EFS021 (Δ*fliN*) and EFS011 (Δ*fliM*) cells were used for the production of rotor subunits.
[b,c] EFS022 (Δ*fliN fliC-sticky*) and EFS012 (Δ*fliM fliC-sticky*) cells were used for the production of rotor subunits. Rotational speed and CCW bias (fraction of time rotating CCW for 1 min) of motor were measured via polystyrene bead attached to flagellum.
[d] Intensity of fluorescent spot at the rotational center of tethered cell. EFS022 and EFS012 cells were used for the production of rotor subunits. Values were shown as arbitrarily unit defined by EMCCD camera.

detected using Alkaline Phosphatase-conjugated anti-mouse IgG antibody and AP conjugate substrate kit (Bio-Rad, USA).

3. Results

3.1. Function of GFP-FliN and FliM-GFP

To express GFP-fused rotor proteins, *gfp* was fused to the 5′ end of *fliN* to form *gfp-fliN*, and to the 3′ end of *fliM* to form *fliM-gfp*. The genes were placed under the control of an arabinose-inducible promoter in plasmids. The swimming speeds of cell producing GFP-FliN and cell producing FliM-GFP were 27.6 and 25.9 μm/s, respectively (Table 1). These values were comparable in cells producing each wild-type subunit. We measured the rotation of motor incorporating each GFP-fusion via small polystyrene bead attached flagellar filament. The rotational speed and CCW bias of the motor incorporating GFP-FliN were 83.2 Hz and 0.67. On the other hand, the rotational speed and CCW bias of the motor incorporating FliM-GFP were 75.7 Hz and 0.58. These values were comparable in a cell producing each wild-type subunit (Table 1). By the immunoblot analysis for whole-cell extracts, in the Δ*fliN* cell producing GFP-FliN, high and weak intensity bands were detected near 40 and 35 kD, respectively (Fig. 1B, lane 3). Because the predicted molecular size of GFP-FliN is 43 kD, the mature form of GFP-FliN probably corresponds to the high intensity band. Weak intensity band near 35 kD might be the digested product in this fusion. In the Δ*fliM* cells producing FliM-GFP, the single band was detected near the predicted molecular size (65 kD) (Fig. 1B, lane 4). To investigate whether each GFP-fusion is incorporated into flagellar motor, we observed the localization of each GFP-fusion in tethered cell using TIRF microscopy. As shown in previous study, in Δ*fliG* cells producing GFP-FliG, single fluorescent spot was detected at the rotational center of tethered cells (Fig. 1C, top) [18]. Similarly, in Δ*fliN* cells producing GFP-FliN and in Δ*fliM* cells producing FliM-GFP, single fluorescent spot was detected at the rotational center of each tethered cell (Fig. 1C, middle and bottom). The fluorescence intensity of motor incorporating GFP-FliN was 3.6-fold higher than those of motor incorporating FliM-GFP (Table 1), which was consistent with the stoichiometry of these subunits in a flagellar motor [2]. These results strongly suggest that each GFP-fusion is functionally incorporated into flagellar motor and allows near wild type motility in each strain.

Table 2
Diffusion coefficient and number of fluorescent spot.

Fusion	Diffusion coefficient (μm²/s)	Number of spots/cell
GFP-FliN	0.0032 ± 0.0013 (n = 9)	3.0 ± 1.9 (0.8 immobile spots)
FliM-GFP	0.010 ± 0.0065 (n = 15)	3.1 ± 1.4 (0.9 immobile spots)
GFP-FliG	0.0053 ± 0.0028 (n = 12)	3.9 ± 2.0 (1.6 immobile spots)

n is the total number of cells that were analyzed. Values were shown as means ± SD.

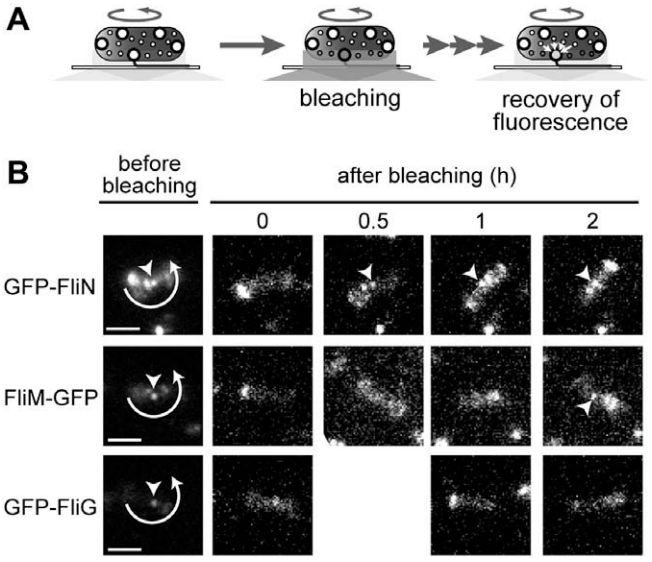

Fig. 2. FRAP experiment for the motor with GFP-fused rotor subunits. (A) Schematic diagrams illustrating the concept of FRAP experiment. A cell is immobilized on the coverslip via a sticky flagellar filament. The cell body rotates around the motor present at the base of the flagellum. Large white circles indicate the flagellar motor with fluorescent GFP-fusions, and small white circles indicate the fluorescent GFP-fusions diffusing in cytoplasm. Evanescent light for observation and photobleaching depicted at the bottom surface of the tethered cell by light gray and dark gray, respectively. The fluorescent spot at the rotational center of the cell and GFP-fusions diffusing near the bottom surface were photobleached (large gray circle and small gray circles). (B) Images before bleaching, 0, 0.5, 1, and 2 h after photobleaching were shown. Images of before bleaching were depicted as relatively wide range of brightness than the other images to show the fluorescent spot at the rotational center of the tethered cell. White arrowheads and circular arrows indicate the fluorescent spots at the rotational center and the rotational direction of cells, respectively. Top, EFS021 cell producing GFP-FliN; middle, EFS011 cell producing FliM-GFP; bottom, DFB225 cell producing GFP-FliG. Scale bar, 1.6 μm.

3.2. Number of fluorescent spots in a cell expressing GFP-fusions in a single bacterial cell

When we observed cells stuck to the coverslip under TIRF microscopy, diffusive motion of fluorescent spots in cytoplasmic membrane was observed in both cells producing GFP-FliN and producing FliM-GFP (Supplementary figure). The estimated diffusion coefficients of fluorescent spots derived from each GFP-fusion were consistent with our previous results (Table 2) [18]. In all strains, approximately one immobile spot was observed (Table 2). In our TIRF microscopy, about one sixth of the surface area of cell was irradiated by evanescent light. This indicates that approximately 6 immobile spots present in one cell, which number is consistent with the average number of flagella per cell for *E. coli*. Therefore, the immobile spots would correspond to mature flagellar basal bodies.

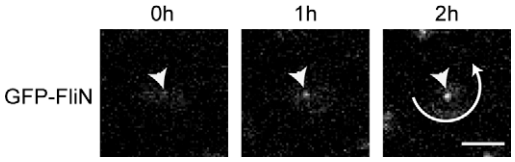

Fig. 3. Co-expression of fluorescent and non-fluorescent GFP-fusions. Images of the same tethered cell were shown every 1 h. Scale bar, 1.6 μm. Details of experimental procedures were described in text.

3.3. Exchange of rotor proteins in functioning flagellar motor

To investigate whether the rotor components are static or dynamic in a rotating motor, we performed FRAP experiment using TIRF microscopy (Fig. 2A). In Δ*fliN* cell producing GFP-FliN, a weak fluorescent spot was observed again at the rotational center 0.5 h later from the bleaching. This fluorescent spot was observed more clearly 1 h later (Fig. 2B, top and Supplementary movie S1–S3). In Δ*fliM* cell producing FliM-GFP, the fluorescent spot was observed again 2 h later from the bleaching (Fig. 2B, middle and Supplementary movie S4–S6). However, in Δ*fliG* cell producing GFP-FliG, the fluorescence at the rotational center did not recovered by the end of observation (2 h) (Fig. 2B, bottom and Supplementary movie S7 and S8). These results suggest that the recovery of fluorescence was caused by the exchange of rotor subunits from bleached one to fluorescent one.

To confirm whether the recovery of fluorescence after photobleaching was caused by the exchange of subunits, the exchange was confirmed by the following experiment (co-production experiment). In Δ*fliN* cells, non-fluorescent GFP(Y66G)-FliN was firstly produced for 4.75 h and fluorescent GFP-FliN was secondly produced for the last 15 min of growth, and then the localization of fluorescent spot at the rotational center was observed. For the first observation, we chose the tethered cell that had a fluorescent spot with low intensity at the rotational center. In this cell, the fluorescent intensity at the rotational center increased with time (Fig. 3 and Supplementary movie S9 and S10). This result suggests that the number of fluorescent subunits in the rotor would increase by the exchange with non-fluorescent subunits. Therefore, results of co-production and FRAP experiments indicate that several kinds of rotor components are exchanged even in a rotating motor. Cells producing non-fluorescent or fluorescent GFP-FliN swam in similar speeds, and the tethered cell producing either GFP-fusion rotated in similar angular velocity (data not shown). These results indicate non-fluorescent and fluorescent GFP-FliN retain comparable function. Therefore, the Y66G mutation into GFP would not affect to the turnover of subunits.

3.4. Recovery of fluorescence in a functioning flagellar motor after partial photobleaching

In order to estimate the exchange-rate of FliN subunit, we partially photobleached the GFP-fusions at the motor and observed the fluorescent transitions of motor with GFP-FliN. After 5 s bleaching, fluorescence of the spot decreased to 23% of the value before bleaching, and recovered up to 36% in 2 h later from bleaching procedure (Fig. 4A, triangles). The shape of the curve in 5 s bleaching was similar to that of the curve in full bleaching procedure (Fig. 4A, circles). On the other hand, after 2 s bleaching, the intensity of the fluorescent spot decreased to 57% immediately after bleaching and decreased to 37% in 2 h later from bleaching procedure (Fig. 4A, squares). Because the rotational speeds of tethered cells before and after bleaching were comparable, the cells would not be suffered damage by the irradiation of evanescent light (Fig. 4B). The estimated dissociation rates in full, 5 and 2 s bleaching procedures were similar, which were calculated as

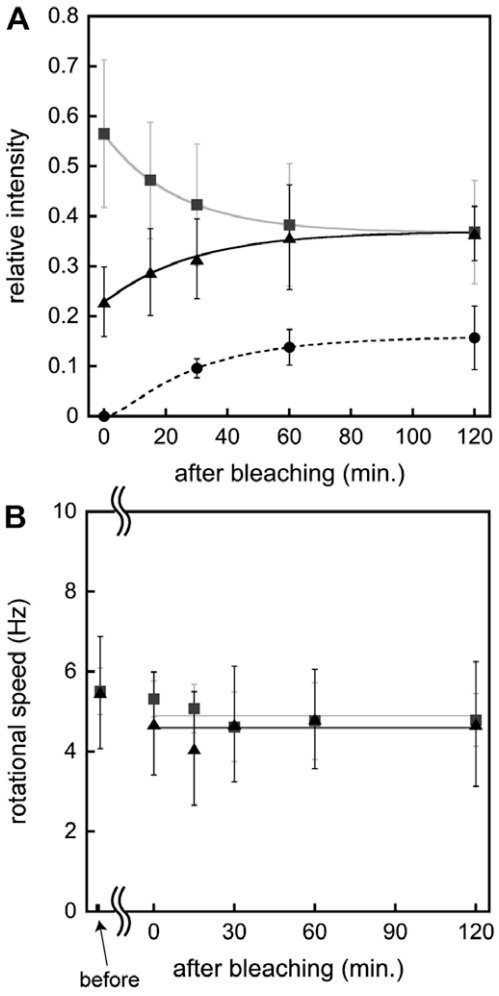

Fig. 4. (A) Transition of fluorescence intensity after full or partial bleaching of motor with GFP-FliN. Fluorescence intensities were normalized by the average value estimated from all samples before bleaching. Triangles, squares, and circles indicate the transitions of fluorescence intensities at the rotational center of tethered cells after 5 s ($n = 12$), 2 s ($n = 7$) and full bleaching ($n = 4$), respectively. For measurements, EFS021 cells harboring pFSGN3 and pYS11, and EFS022 cells harboring pFSGN3 were used. In both strain, there were no difference in the transitions of fluorescence intensity. (B) Average rotational speed of tethered cells after 5 and 2 s bleaching. Triangles and squares indicate the rotational speeds of tethered cells in the 5 and 2 s bleaching experiments, respectively. Black and gray lines are the average rotational speed after 5 and 2 s bleaching, respectively. Arrow indicates the rotational speed of tethered cells before bleaching.

$0.0008\ s^{-1}$, 0.0006 and $0.0007\ s^{-1}$, respectively (see discussion). These results suggest that FliN subunits are exchanged in tens of minutes, and the turnover rate of FliN subunit is independent of the photobleaching ratio.

4. Discussion

While the overall structure of flagellar motor has been thought to be static, the dynamic behavior of the stators is reported recently [5,16,17]. In the present study, we focused on the dynamics of the rotor components in a functioning motor. In FRAP experiments to the motor incorporating GFP-FliN or FliM-GFP, the recovery of fluorescence was observed (Fig. 2B). Because the fluorescence of the motor incorporating GFP-FliG did not recovered after bleaching, the recovery of fluorescence is probably not due to the reformation of chromophore of GFP. Therefore, the recovery of fluorescence strongly suggests that rotor subunits, FliN and FliM, are exchanged even in the rotating motor. The result of the co-pro-

duction of non-fluorescent and fluorescent GFP-FliN also indicates the exchange of rotor subunits in the rotating motor. Biochemical analysis showed the formation of a $FliM_1FliN_4$ complex [19], however, the turnover of FliM-exchange was slower than that of FliN subunits in our FRAP experiment. Therefore, the exchange of FliN would be mainly independent of FliM. FliN also interacts with FliH, which is a component of export apparatus [20]. The association/dissociation of components of export apparatus might be involved in the exchange of FliN subunits. In the model proposed by Brown et al., ring-shaped tetramer of FliN is arranged at the circular domain locating at the most bottom of the C-ring and FliM is arranged between FliG and FliN [21]. The slower rate of FliM-exchange could be explained by the location of this subunit in the motor. Other group (Prof. J. Armitage, personal communication) has observed the exchange of FliM subunit. The exchange of this subunit appeared to depend on the presence of phosphorylated CheY. The turnover rate of FliM might be varied via chemotactic system that responds to extracellular signal. In our study, the exchange of FliG subunits was not observed. It was shown that functional flagellar motor are constructed by the fused protein of FliF and FliG, and suggested that FliG has the same symmetry-fold as the MS-ring rather than that of the C-ring [22,23]. Also, FliG subunits were isolated from flagellar basal body of *Vibrio alginolyticus*, however, FliM subunit was not [24]. These studies suggest that FliG tightly bound to MS-ring rather than to FliM. Therefore, FliG subunits would not be exchanged for at least 2 h.

To estimate the turnover rate of GFP-FliN, the transitions of fluorescence intensity at the motor were fitted by the kinetic scheme (Fig. 4A) (details were described in Supplementary materials). The dissociation rates in full, 5 and 2 s bleaching procedures were calculated as 0.0008, 0.0006 and 0.0007 s^{-1}, respectively. These values indicate that FliN is exchanged in tens of minutes. This time scale of dissociation rate is 50-fold slower than that of stator units, which dissociation rate was 0.04 s^{-1} [17]. Difference of dissociation rate would be due to the role of each component in flagellar rotation. Stator unit not only generates torque of motor rotation but also directly regulates the function of motor via its association/dissociation in response to extracellular environment [16]. To response to extracellular environment expeditiously, the more frequent replacement than that of rotor components would be required. On the other hand, the rotor is a structure receiving the torque generated by stators. Therefore, the exchanges of stator units and of rotor subunits would have intrinsically different significance. Though the physiological meaning of the subunit-exchange of the rotor is not clear, the cells might keep the flagellar motor functional by the replacement of rotor subunit to compensate for protein damage or incorporation of defective subunits. The exchange of rotor subunits might be an advantage for growth as energy would be spent on growth rather than constructing new flagella.

Why did the fluorescence intensity at the motor decrease after 2 s bleaching and increase after 5 s bleaching? If the ratio of photobleaching by irradiation of evanescent light was similar both in the motor and in the cytoplasm, the recovery of fluorescence should show similar tendency in both bleaching procedure. The presumable interpretation is that the bleaching ratio by the evanescent light in the motor and in the cytoplasm would not be the same because the environmental conditions, such as pH, hydrophobicity, and the interaction to another molecules, were different between in the motor and in the cytoplasm. Actually, the degree of bleaching to the cell background (cytoplasm) and to the motors was different by the bleaching time (data not shown). Therefore, the transition phase of fluorescence intensity after 2 and 5 s bleaching would be varied because the proportion of each state (see kinetic scheme in Supplementary materials) and the proportion of photobleached and fluorescent subunits in cytoplasm were different by the bleaching time.

We demonstrated the subunit-exchange of rotor components in a rotating bacterial flagellar motor. These novel findings indicate that supramolecular machines, such as the bacterial flagellar motor, are not static structures but the subunits in a molecular machine are dynamically exchanged even in functioning state. Thus, these kinds of machines could function tolerating the exchange of subunits. In contrast to the man-made machines, this flexibility might be the important property for sustaining the function of molecular machines constructed by living organisms. We have to clarify how the exchange of rotor subunits involves in the motor function as a future work.

Acknowledgments

We thank Prof. Michio Homma for the gift of some bacterial strains and discussion, and Prof. Takeharu Nagai and Dr. Kenta Saito for the gift of some plasmids encoding GFP variant. Also we thank Prof. Judith Armitage, Dr. Richard Berry, and Dr. Nicolas Delalez for useful discussion. This work was supported by Grants-in-Aid for Scientific Research from The Ministry of Education, Culture, Sports, Science and Technology and from the Japan Society for the Promotion of Science (to H.F. and A.I.).

Appendix A. Supplementary data

Supplementary data associated with this article can be found, in the online version, at doi:10.1016/j.bbrc.2010.02.129.

References

[1] M.D. Manson, P. Tedesco, H.C. Berg, F.M. Harold, C. van der Drift, A proton motive force drives bacterial flagella, Proc. Natl. Acad. Sci. USA 74 (1977) 3060–3064.
[2] D.F. Blair, Flagellar movement driven by proton translocation, FEBS Lett. 545 (2003) 86–95.
[3] T. Yorimitsu, M. Homma, Na^+-driven flagellar motor of *Vibrio*, Biochim. Biophys. Acta 1505 (2001) 82–93.
[4] M. Ito, D.B. Hicks, T.M. Henkin, A.A. Guffanti, B.D. Powers, L. Zvi, K. Uematsu, T.A. Krulwich, MotPS is the stator-force generator for motility of alkaliphilic *Bacillus*, and its homologue is a second functional Mot in *Bacillus subtilis*, Mol. Microbiol. 53 (2004) 1035–1049.
[5] A. Paulick, A. Koerdt, J. Lassak, S. Huntley, I. Wilms, F. Narberhaus, K.M. Thormann, Two different stator systems drive a single polar flagellum in *Shewanella oneidensis* MR-1, Mol. Microbiol. 71 (2009) 836–850.
[6] W.S. Ryu, R.M. Berry, H.C. Berg, Torque-generating units of the flagellar motor of *Escherichia coli* have a high duty ratio, Nature 403 (2000) 444–447.
[7] Y. Sowa, H. Hotta, M. Homma, A. Ishijima, Torque-speed relationship of the Na^+-driven flagellar motor of *Vibrio alginolyticus*, J. Mol. Biol. 327 (2003) 1043–1051.
[8] Y. Inoue, C.J. Lo, H. Fukuoka, H. Takahashi, Y. Sowa, T. Pilizota, G.H. Wadhams, M. Homma, R.M. Berry, A. Ishijima, Torque-speed relationships of Na^+-driven chimeric flagellar motors in *Escherichia coli*, J. Mol. Biol. 376 (2008) 1251–1259.
[9] S.W. Reid, M.C. Leake, J.H. Chandler, C.J. Lo, J.P. Armitage, R.M. Berry, The maximum number of torque-generating units in the flagellar motor of *Escherichia coli* is at least 11, Proc. Natl. Acad. Sci. USA 103 (2006) 8066–8071.
[10] T. Yorimitsu, M. Kojima, T. Yakushi, M. Homma, Multimeric structure of the PomA/PomB channel complex in the Na^+-driven flagellar motor of *Vibrio alginolyticus*, J. Biochem. 135 (2004) 43–51.
[11] H. Fukuoka, T. Yakushi, A. Kusumoto, M. Homma, Assembly of motor proteins, PomA and PomB, in the Na^+-driven stator of the flagellar motor, J. Mol. Biol. 351 (2005) 707–717.
[12] S. Kojima, K. Imada, M. Sakuma, Y. Sudo, C. Kojima, T. Minamino, M. Homma, K. Namba, Stator assembly and activation mechanism of the flagellar motor by the periplasmic region of MotB, Mol. Microbiol. 73 (2009) 710–718.
[13] J.D. Zhou, S.A. Lloyd, D.F. Blair, Electrostatic interactions between rotor and stator in the bacterial flagellar motor, Proc. Natl. Acad. Sci. USA 95 (1998) 6436–6441.
[14] A. Bren, M. Eisenbach, The N terminus of the flagellar switch protein, FliM, is the binding domain for the chemotactic response regulator, CheY, J. Mol. Biol. 278 (1998) 507–514.
[15] M.A. Mathews, H.L. Tang, D.F. Blair, Domain analysis of the FliM protein of *Escherichia coli*, J. Bacteriol. 180 (1998) 5580–5590.
[16] H. Fukuoka, T. Wada, S. Kojima, A. Ishijima, M. Homma, Sodium-dependent dynamic assembly of membrane complexes in sodium-driven flagellar motors, Mol. Microbiol. 71 (2009) 825–835.

[17] M.C. Leake, J.H. Chandler, G.H. Wadhams, F. Bai, R.M. Berry, J.P. Armitage, Stoichiometry and turnover in single, functioning membrane protein complexes, Nature 443 (2006) 355–358.
[18] H. Fukuoka, Y. Sowa, S. Kojima, A. Ishijima, M. Homma, Visualization of functional rotor proteins of the bacterial flagellar motor in the cell membrane, J. Mol. Biol. 367 (2007) 692–701.
[19] P.N. Brown, M.A. Mathews, L.A. Joss, C.P. Hill, D.F. Blair, Crystal structure of the flagellar rotor protein FliN from *Thermotoga maritima*, J. Bacteriol. 187 (2005) 2890–2902.
[20] B. González-Pedrajo, T. Minamino, M. Kihara, K. Namba, Interactions between C ring proteins and export apparatus components: a possible mechanism for facilitating type III protein export, Mol. Microbiol. 60 (2006) 984–998.
[21] P.N. Brown, M. Terrazas, K. Paul, D.F. Blair, Mutational analysis of the flagellar protein FliG: sites of interaction with FliM and implications for organization of the switch complex, J. Bacteriol. 189 (2007) 305–312.
[22] H. Suzuki, K. Yonekura, K. Namba, Structure of the rotor of the bacterial flagellar motor revealed by electron cryomicroscopy and single-particle image analysis, J. Mol. Biol. 337 (2004) 105–113.
[23] D.R. Thomas, N.R. Francis, C. Xu, D.J. DeRosier, The three-dimensional structure of the flagellar rotor from a clockwise-locked mutant of *Salmonella enterica* serovar Typhimurium, J. Bacteriol. 188 (2006) 7039–7048.
[24] M. Koike, H. Terashima, S. Kojima, M. Homma, Isolation of basal bodies with C-ring components from the Na^+-driven flagellar motor of *Vibrio alginolyticus*, J. Bacteriol. 192 (2010) 375–378.